Rotational structure of highly deformed ^{99}Y: Decay of ^{99}Sr

R. F. Petry and H. Dejbakhsh*
University of Oklahoma, Norman, Oklahoma, 73019

John C. Hill and F. K. Wohn
Ames Laboratory and Iowa State University, Ames, Iowa 50011

M. Shmid† and R. L. Gill
Brookhaven National Laboratory, Upton, New York 11973
(Received 16 July 1984)

The level structure of the $N=60$ isotone ^{99}Y has been studied via the decay of ^{99}Sr. γ singles and γ-γ coincidence measurements have resulted in 71 γ transitions placed in a decay scheme with 26 levels. γ-ray multiscaling measurements give a ^{99}Sr half-life of 270±10 ms. Five rotational bands, including the previously identified $K=\frac{5}{2}$ ground-state band, have been identified in ^{99}Y. Nilsson orbitals, with bandhead energies in keV in parentheses, associated with these five bands are $\frac{5}{2}$[422] (0), $\frac{5}{2}$[303] (487), $\frac{3}{2}$[301] (536), $\frac{1}{2}$ [431] (1011), and $\frac{3}{2}$[431] (1119). The rotational features are consistent with an axially symmetric deformation in the range 0.3 to 0.4. The characteristics of these bands and their associated γ-ray transitions are discussed.

I. INTRODUCTION

Evidence for six rotational bands in four odd-A nuclei in the $A\simeq100$ region has been given in a previous publication.[1] One of these nuclei was ^{99}Y for which a $K=\frac{5}{2}$ ground-state band was identified and associated with the Nilsson orbital $\frac{5}{2}$[422]. It is the purpose of this paper to present the details of the study of the decay of ^{99}Sr to levels in ^{99}Y. The following paper (paper II) presents calculations of the rotational band structure of ^{99}Y.

The region of interest on the nuclide chart lies on the neutron-rich side of the valley of stability and is bounded by $28<Z<50$ and $N>50$. Stable deformations were predicted for this region by Arseniev *et al.*[2] in 1969. The first experimental evidence for these deformations was found by Cheifetz *et al.*[3,4] in their study of ^{252}Cf fission fragments. They observed rotational bands in even-even nuclei with greatly enhanced $B(E2)$ values consistent with equilibrium deformations β in the range 0.3—0.4. There followed extensive nuclear spectroscopic studies of the level structure of the even-even isotopes of Sr, Zr, Mo, and Ru, mostly from the investigation of the decay of fission products produced at ISOL (isotope separator on-line) facilities. The results of these studies are summarized in Refs. 5—7. β values of 0.34 for ^{98}Sr, 0.36 for ^{100}Sr, and 0.32 for ^{100}Zr have been deduced from $B(E2)$ measurements.[5,6]

In Fig. 1 the energy systematics of the 2_1^+ state and the $E(4_1^+)/E(2_1^+)$ ratio are plotted for nuclides in the $A\simeq100$ region as a function of Z and N. For even-even nuclei it is clear from the behavior of the 2_1^+ levels that a nuclear shape transition occurs as neutrons are added beyond $N=58$, and that this transition becomes extremely sharp for $Z\leq40$. The $E(4_1^+)/E(2_1^+)$ ratio approaches the value of 10/3 characteristic of an axially symmetric rigid rotor for Sr and Zr isotopes with $N\geq60$. For the heavy even-A Ru and Pd isotopes, experimental evidence can be best explained if these nuclei have basically a γ-unstable character.[7] Further evidence for the transitional nature of the $N=60$ isotones of Sr and Zr comes from the systematics of the 0_2^+ level which is exceptionally low at $N=60$ but is much higher for lower values of N.

Potential energy calculations[8–11] indicate prolate minima at deformations in the range 0.3—0.4 for $N\geq60$ and spherical minima for $N<60$. The calculations in Ref. 8 also predict a tendency toward axial asymmetry in this region. The subshell closure at $N=56$ is reproduced in the calculations of Refs. 10 and 11. For the Ru and Pd isotopes, a successful interpretation of the shape transition has been made within the framework of the interacting boson model (IBM) as a SU(5) to O(6) transition.[12] In the same framework the transition in the Sr and Zr isotopes would be characterized as SU(5) to SU(3). In a different approach Federman and Pittel[13] have proposed a microscopic shell model description of the shape transition in which deformation occurs because of the domination for spin orbit partners (SOP) of the n-p force over the n-n and p-p pairing force. They successfully predict the shape transition at $N=60$ in calculations on the Zr and Mo isotopes where they are able to describe the behavior of the 0_2^+ level as a function of neutron number.

The study of the even-even nuclides in this region has thus provided a picture of nuclear shapes that is similar to, but more dramatic than, that found in the rare-earth region. In the lower-Z range clear evidence is found for stable prolate deformations and a transition boundary at $N=60$, similar to the situation encountered for $N=90$ in the rare earths. As Z increases toward the upper end of the region the transition nuclei become γ soft and/or triaxial, much as they do in the heavier mass region for the

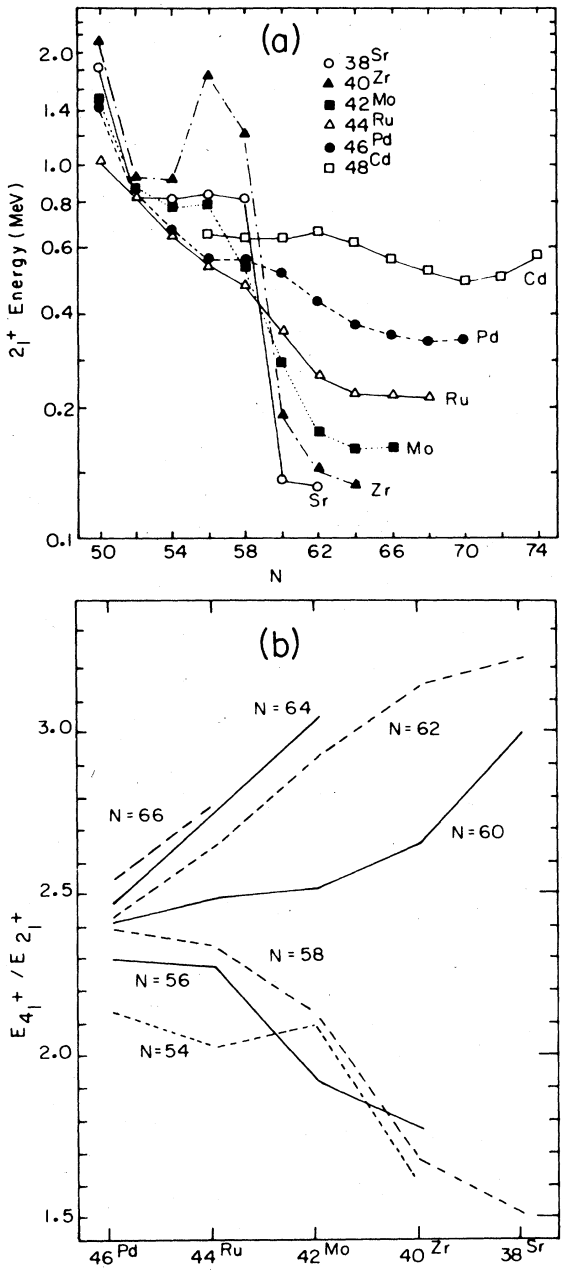

FIG. 1. Systematics of even-even nuclei in the $A \simeq 100$ region.

Pt isotopes. The main difference between the $A \simeq 100$ and rare-earth regions is the sharpness of the shape transition in the $A \simeq 100$ region (it occurs in a much narrower range of Z and N) and the apparent coexistence of nearly spherical and highly prolate shapes (i.e., the exceptionally low 0_2^+ levels for ^{98}Sr and ^{100}Zr at $N=60$). The systematics of the excited 0^+ states are summarized in Ref. 9. Both effects appear to be closely related to the $N=56$ neutron subshell closure.[10,11] According to Bengtsson *et al.*,[11] the combination $Z=38,40$ and $N=56$ give a particularly low shell energy for the spherical shape with the result that the onset of deformation is much sharper for Sr and Zr.

A clear gap in the study of this region is the lack of information on single particle states in deformed nuclei with $N \geq 60$. Such information has played a crucial role in the understanding of the rare-earth nuclei.[14] When the present experiment began there existed no published information on Nilsson assignments for levels in deformed odd-A Sr, Y, or Zr nuclei with $N \geq 60$, although Pfeiffer *et al.*[15] reported a preliminary study of the decay of ^{99}Sr during the course of the present work. Data were available from direct mass measurements[16] on the Rb isotopes from which one- and two-neutron separation energies could be extracted. A hump in these curves at $N=60$ is similar to those observed in the rare-earth[17] and neutron-rich Na isotopes.[18] This behavior is associated with the shape transition in these regions. Also available were optical measurements of the quadrupole moment and isotope shift for ^{97}Rb which lead to a deformation $\beta=0.33$,[19] consistent with the β values for ^{98,100}Sr.[5,6]

Spectroscopic studies of these nuclides must of necessity be made from experiments on beta-decaying fission products, since the use of single-nucleon transfer reactions (which was so effective in the rare-earth region) is impossible for neutron-rich deformed nuclei in the $A \simeq 100$ region. From studies of the decay of an 8.6-μs isomer[20] in ^{99}Y and our studies of the β decay of ^{99}Sr, we identified the ground and first three excited states of ^{99}Y with a $K=\frac{5}{2}$ rotational band based on the $\frac{5}{2}[422]$ Nilsson single-particle state.[1] Although model dependent, the arguments for these assignments were based on fundamental characteristics of states of odd-A deformed nuclei which have been well established for the rare-earth and other deformed regions.[14] The assignments are also supported by the discovery of rotational bands in neighboring odd-A nuclei with $N \geq 60$. Recently, $\frac{3}{2}[411]$ ground state bands have been identified in $^{103}_{42}Mo_{61}$ and $^{105}_{42}Mo_{63}$ (Ref. 21) and three rotational bands, $\frac{5}{2}[422]$, $\frac{5}{2}[303]$, and $\frac{3}{2}[301]$, have been identified in $^{103}_{41}Nb_{62}$ (Ref. 22).

The present paper gives details of our study of the decay of ^{99}Sr. Section II presents experimental methods and results. The decay scheme is discussed in Sec. III. The

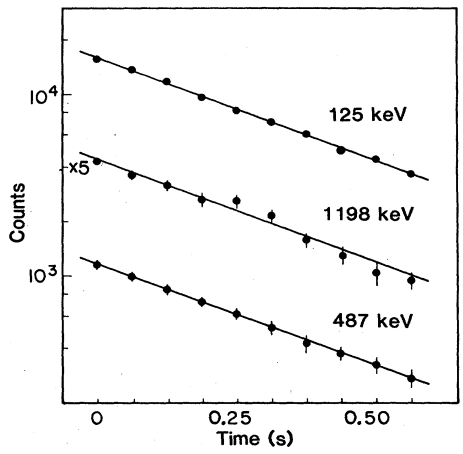

FIG. 2. Sample decay curves for γ rays following the decay of ^{99}Sr. The lines represent fits with a half-life of 0.27 ± 0.01 s.

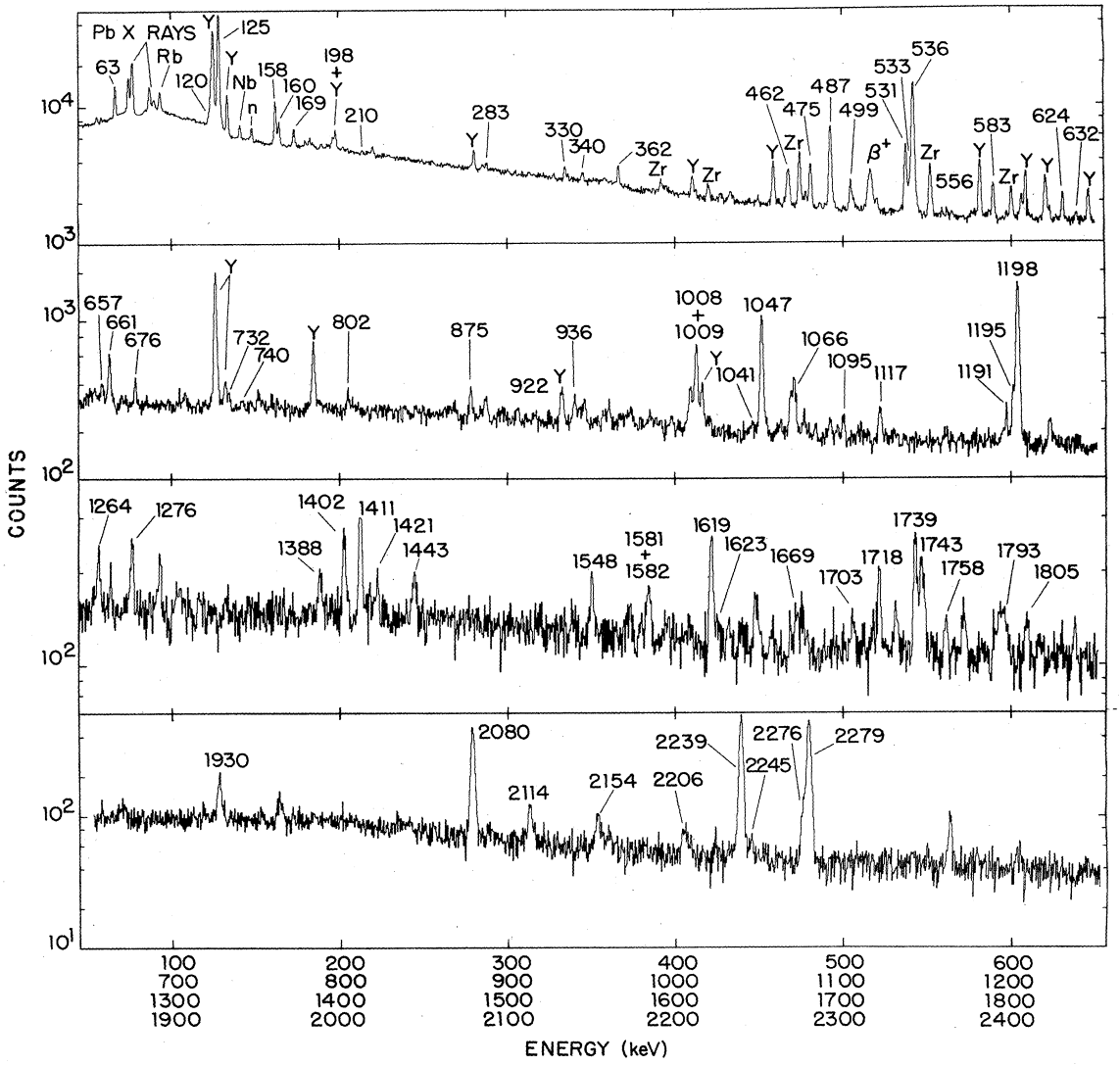

FIG. 3. γ-ray singles spectrum from the decay of a mass 99 source. Lines associated with the decay of ^{99}Sr are labeled by their energies. Known lines following other decays are labeled as follows: ^{99}Rb (Rb), ^{99}Y (Y), ^{99}Zr (Zr), ^{99}Nb (Nb), ^{99}Rb delayed neutron (n). Unlabeled lines are unidentified long-lived γ rays.

observed rotational bands are discussed qualitatively in Sec. IV. The following paper (paper II) presents a particle-rotor calculation of the rotational band structure of ^{99}Y which includes the Coriolis-coupling effects and calculated $E1$, $M1$, and $E2$ transition probabilities.

II. EXPERIMENTAL METHODS AND RESULTS

A. Source preparation

Sources of ^{99}Sr for this study were obtained at the TRISTAN isotope-separator facility operating on-line to the Brookhaven National Laboratory high-flux beam reactor. For the present study a high-temperature Re surface ionization source containing a target of 5 g of enriched ^{235}U was exposed to a neutron flux of 1.5×10^{10} n/cm^{2}s. Positive ion beams of Rb and Sr were extracted from the source, mass separated, and deposited on a movable aluminum-coated Mylar tape. A detailed description of this ion source may be found in Ref. 23.

The use of a Re ionizing surface enhanced the production of primary ^{99}Sr, which dominated the activity collected. Small amounts of ^{99}Rb were also present, and a very small production of primary ^{99}Y cannot be completely ruled out. There was no evidence for cross contamination from adjacent masses. The only γ rays observed from ^{99}Rb decay were the prominent 91-keV line and a γ ray at 144 keV from ^{99}Rb delayed neutron emission which depopulates the 2_1^+ state in ^{98}Sr.

B. Measurements

Gamma-ray measurements were made with one Ge(Li) and one HpGe detector placed in 180° geometry at the point at which the beam was deposited onto the tape. A thin plastic scintillator also viewed the deposit point with

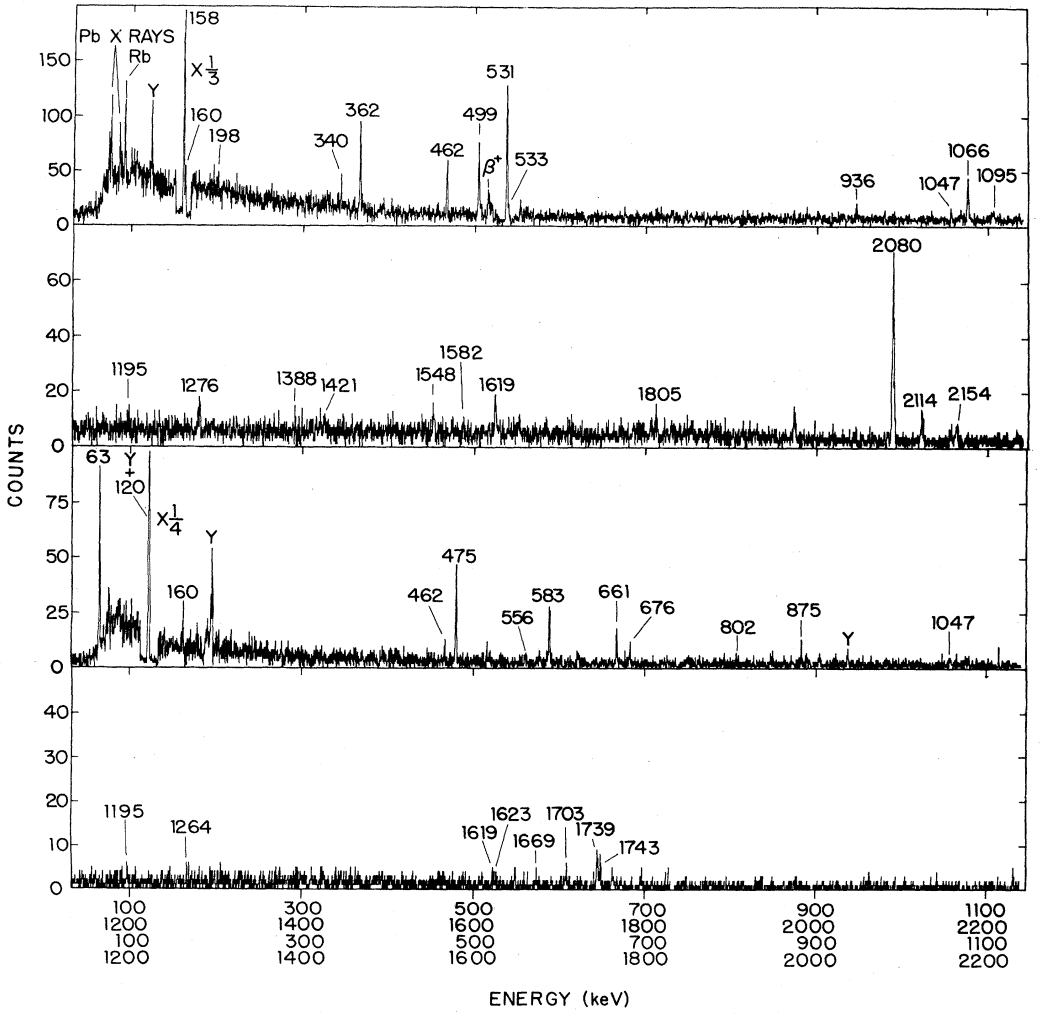

FIG. 4. Coincidence γ-ray spectra from the decay of ^{99}Sr for gates on (a) 125- and (b) 536-keV lines, respectively. Peaks labeled with Y in the 536-keV gate are in coincidence with a 536-keV γ ray following the decay of ^{99}Y.

an acceptance solid angle of approximately π steradians. Signals from this scintillator served as a beam monitor and were also used as a β coincidence gate for some of the singles spectra. Spectra thus gated were free of all background lines except Pb x rays from scattering from the surrounding shielding and possibly the 1293-keV ^{41}Ar line. Enhancement of ^{99}Sr γ lines relative to those from the ^{99}Y and ^{99}Zr daughters was achieved by moving the tape at short intervals compared to the buildup time for ^{99}Y. Sixteen β-gated γ singles spectra were recorded at $\frac{1}{16}$-s intervals during each tape cycle. These multiscale spectra were used for half-life determination and isobar identification. A sum of the 16 spectra provided the spectrum from which γ-ray energies and relative intensities were determined. The first six of these spectra ($\Delta t = \frac{3}{8}$ s) were accumulated with the ion beam on, which permitted observation of the growth of the lines from the different isobars. The last nine spectra ($\Delta t = \frac{9}{16}$ s) were accumulated while the ion beam was deflected and provided the data from which half-lives were determined. This cycle was repeated for a total running time of approximately 80 h. To check the effect of β gating on the γ-ray intensity pattern, a non-β-gated γ singles spectrum was collected simultaneously with the γ multiscale data throughout the experiment.

The energy range covered by both the coincidence and singles experiments was 0—3 MeV. To check for transitions above this range, a beta-gated singles spectrum covering energies up to 5.5 MeV was collected for the duration of the experiment. No γ rays associated with ^{99}Sr decay were observed above 2.5 MeV. The energy calibration of the system was made by simultaneous measurements of γ rays from the $A=99$ decay chain and a set of standard sources. From these data the nonlinearities of the system were determined. Use was also made of the fact that the energies of several lines in the ^{99}Y and ^{99}Zr daughter decay have been measured with high precision on a curved-crystal spectrometer.[24] Finally a spectrum was accumulated with the tape stationary after the source had reached saturation in all isobars through ^{99}Nb, which occurred 15

TABLE I. γ transitions observed in ^{99}Sr decay.

E_γ (keV)	I_γ	Placement (keV)	Coincident γ rays (keV)
63.85±0.08	8.5±0.5	599—536	536
120.58±0.12	11.4±1.0	656—536	160,536,1195,1421,1619
125.12±0.03	100[a]±6	125—0	158,160,(198),340,362,462,499,531,533, 936,1047,1066,1095,1195,1276,1388, (1421),1548,1582,1619,1805,2080, 2114,2154
158.62±0.04	10.7±0.7	283—125	125,340,533,936
160.73±0.04	4.6±0.4	817—656	120,125,169,531,536,1388,1421
169.56±0.04	3.2±0.3	656—487	125,160,487
198.47±0.20	0.7±0.2	484—283	125,158
210.05±0.20	0.8±0.1	1402—1191	125,1066,(1191)
283.68±0.13	1.0±0.2	283—0	
330.30±0.11	2.4±0.3	817—487	362,487
340.81±0.12	1.3±0.2	624—283	125,158,(283)
362.11±0.05	3.0±0.2	487—125	125
395[b]	<0.8	1213—817	
462.70±0.06	6.3±0.6	1119—656	120,125,169,(487),531,536,1195
475.59±0.05	8.5±0.6	1011—536	536,1264
487.31±0.05	28.5±1.8	487—0	169,330,1443,1718,(1793)
499.26±0.07	4.8±0.5	624—125	125,(1581)
531.75±0.06	18.7±1.5	656—125	125,160,462,(556),1195,(1582),1619
533.9±0.3	4.3±1.4	817—283	125,158
536.12±0.05	87±7[c]	536—0	63,120,160,462,475,556,583,661,676, (802),875,1047,1195,1264,(1619),(1622), (1669),1703,1739,1743
556.4 ±0.3	0.8±0.3	1213—656	
583.43±0.05	6.0±0.4	1119—536	536,1195
589[b]	<0.5	1213—624	
624.32±0.06	4.6±0.3	624—0	(1581)
632.32±0.19	1.7±0.2	1119—487	487
657.17±0.16	2.0±0.2	656—0	
661.58±0.07	5.5±0.4	1197—536	536,1047
676.87±0.08	2.2±0.2	1213—536	
692[b]	<0.6	817—125	
726[b]	<1.5	1213—487	
732.3 ±0.3	1.5±0.2	1930—1197	
740.1 ±1.0	0.9±0.2	1930—1191	1191
802.7 ±0.3	1.1±0.2	1402—599	63,536
817[b]	<0.4	817—0	
875.44±0.12	3.3±0.4	1411—536	536
922.0±0.3	0.9±0.3	1930—1009	
936.93±0.11	2.8±0.3	1220—283	125,158
1008.00±0.20	3.1±0.6	2205—1197	1198
1009.12±0.20	10.8±0.8	1009—0	
1041.7 ±0.4	1.0±0.3	2239—1197	
1047.35±0.08	26.1±1.8	2245—1197	536,661,1198
1066.48±0.20	8.4±0.8	1191—125	125,210
1088[b]	<1.0	1213—125	
1095.52±0.15	3.8±0.4	1220—125	125
1117.1 ±0.3	4.6±0.4	2314—1197	1198
1119[b]	<1.0	1119—0	
1191.28—0.20	3.5±0.5	1191—0	210
1195.28±0.18	6.1±1.3	2314—1119	120,125,462,531,536,583
1198.12±0.08	57 ±4	1197—0	1007,(1009),1047,1117
1213[b]	<1.0	1213—0	
1264.62±0.22	1.9±0.3	2276—1011	536
1276.95±0.13	4.5±0.5	1402—125	125
1388.44±0.23	3.6±0.6	2205—817	(120),125,160,487,(531)
1402.16±0.15	7.4±0.8	1402—0	
1411.74±0.12	10.1±0.8	1411—0	

TABLE I. (*Continued*).

E_γ (keV)	I_γ	Placement (keV)	Coincident γ rays (keV)
1421.54±0.18	3.0±0.4	2239—817	125,(160),169,536
1443.44±0.18	4.4±0.5	1930—487	(125),487
1548.89±0.18	5.2±0.7	2205—656	(120),125
1581.0 ±0.4	2.3±0.3	2205—624	120,125,(531),536
1582.6 ±0.3	3.0±0.3	2239—656	
1619.23±0.13	9.8±0.9	2276—656	120,125,531,536
1623.0 ±0.3	2.0±0.4	2279—656	536
1669.8 ±0.3	2.9±0.7	2205—536	536
1703.28±0.18	2.9±0.3	2239—536	536
1718.84±0.16	5.6±0.6	2205—487	487
1739.82±0.15	9.5±0.8	2276—536	536
1743.6 ±0.4[d]	7 ±3[d]	2279—536	
1758.14±0.17	4.6±0.4	2245—487	487
1793.0 ±0.4	4.4±0.9	2279—487	(487)
1805.72±0.24	6.5±0.8	1930—125	125
1930.68±0.20	9.3±0.8	1930—0	
2080.38±0.20	35 ±3	2205—125	125
2114.40±0.21	6.5±0.7	2239—125	125
2154.6 ±0.3	6.0±1.0	2279—125	125
2206.1 ±0.3	4.3±0.5	2205—0	
2239.28±0.20	46 ±3	2239—0	
2245.3 ±0.3	2.2±0.5	2245—0	
2276.00±0.22	7.3±1.5	2276—0	
2279.42±0.20	47 ±3	2279—0	

[a]Intensities normalized to 100 for the 125-keV γ ray.
[b] No γ ray observed; only an upper limit on I_γ could be set.
[c]Intensity corrected for contribution from ^{99}Y decay.
[d]Energy and intensity from spectrum in coincidence with 536-keV γ ray. The 1743-keV γ ray contains a long-lived (not ^{99}Sr) component.

min after the start of the activity collection. This spectrum was used along with some absolute γ intensities[15,25,26] from the decay of ^{99}Zr to estimate the ground-state β branch in the decay of ^{99}Sr.

γ-γ coincidence events were recorded on magnetic tape as address triplets representing the γ-ray energies and their time separation. The timing signal was derived from a standard fast coincidence system with (amplitude and rise time compensated) (ARC) timing and time-to-amplitude conversion. Time resolution at FWHM was 20 ns.

C. Half-life

The half-life for the decay of ^{99}Sr was determined by following the decay of strong and reasonably clean γ lines at 63, 125, 487, 1198, 2239, and 2279 keV in the multiscale data. The decay curves for the 125-, 487-, and 1198-keV lines are shown Fig. 2. A weighted average for the above six γ rays yields a mean half-life (with rms uncertainty) of 270±10 ms. Our value is in good agreement with the half-life of 290±40 ms measured by Koglin *et al.*[27] but disagrees with an earlier value[28] of 0.6±0.2 s.

D. γ-ray energies, intensities, and coincidence relationships

The γ-ray spectrum obtained from the sum of the multiscale data is given in Fig. 3. The spectrum is free of background lines (except possibly the 1293-keV line from ^{41}Ar) because of the β-gate condition imposed on it. In Fig. 4 γ-ray spectra in coincidence with the 125- and 536-keV γ rays are shown. The γ energies, relative intensities, placements, and coincidence relationships among the γ transitions are summarized in Table I. The uncertainties associated with the energies are due to statistical uncertainties in determining peak centroids and system nonlinearities, while the uncertainties associated with the relative intensities reflect uncertainties in the determination of peak areas and detector efficiencies. Comparison of relative peak areas from this spectrum with those from a spectrum from the same detector that was not β gated indicates no measureable distortion of intensities as a result of β gating.

Determination of the characteristics of the 536-keV line required some special consideration. The line coincides almost exactly in energy to a transition following the decay[25] of ^{99}Y, but its intensity in the ^{99}Sr-enhanced spectrum is nearly a factor of 10 larger relative to other ^{99}Y lines than the ratio reported in Ref. 25. That a portion of the strength of this line is associated with the decay of ^{99}Sr is confirmed by the coincidence data, in which the 536-keV γ ray is found to be in coincidence with several ^{99}Sr lines, in particular the strong 63-keV γ ray. To obtain a correction for the ^{99}Y contribution, a delayed spectrum was taken with ^{99}Sr absent to obtain the ratio of the intensity of the 536- to 724-keV line in ^{99}Y decay. The

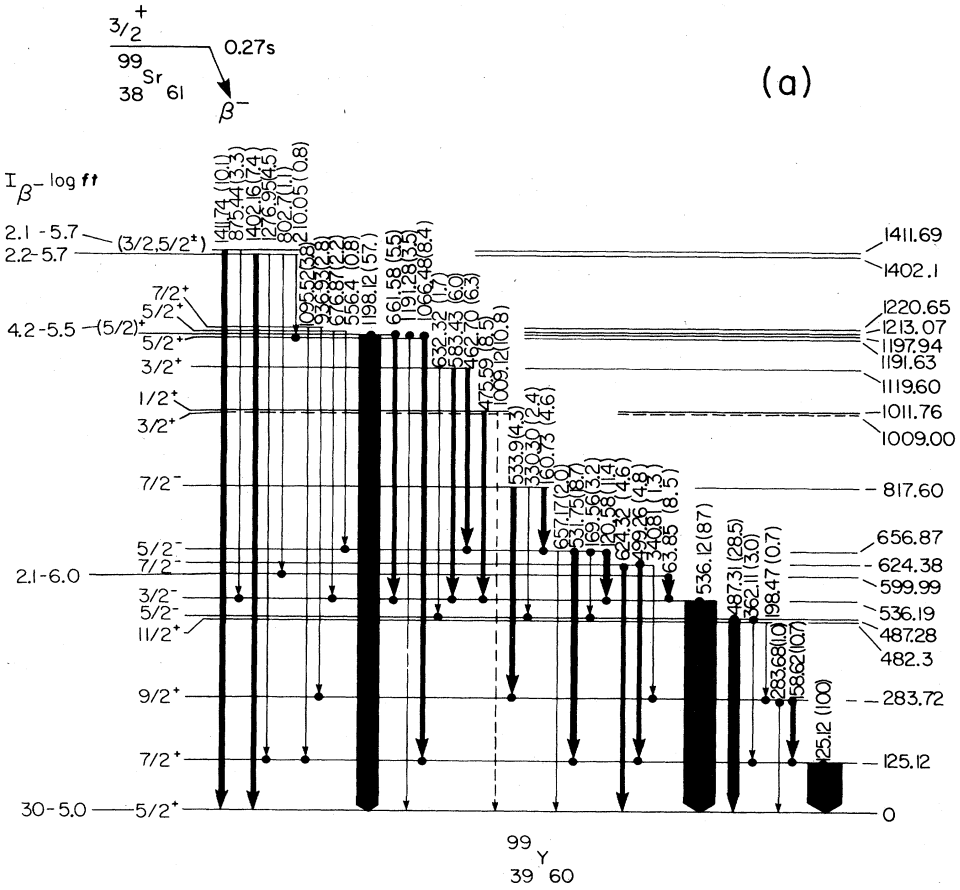

FIG. 5. Decay scheme for ^{99}Sr. β branchings and logft values are shown only for those levels for which the branching $>2.0\%$.

724-keV γ ray from ^{99}Y decay also appears cleanly in the ^{99}Sr spectrum and can be used as a basis for correcting the intensity of the 536-keV line. Application of this technique to the multiscale data allows a half-life associated with the ^{99}Sr portion of this line to be extracted. Before the correction, a fit to the decay data for this line yielded a half-life value of 0.37 s. After the correction, the fit produces a half-life of 0.28 ± 0.02 s, in agreement with data for other strong ^{99}Sr lines.

III. THE ^{99}Sr DECAY SCHEME

The level scheme for ^{99}Y from the decay of ^{99}Sr, based on the γ-ray singles and coincidence measurements, is shown in Fig. 5. Placements for individual γ rays are indicated in Table I. Information on level energies, β feedings, and logft values is summarized in Table II. The β-branching ratios and logft values in Table II were determined from γ-ray intensity balances. A Q_β value of 7.90 ± 0.15 MeV was used.[29]

The ^{99}Sr ground-state β feeding was determined from our saturation spectrum assuming that only Rb and Sr activities were present in the $A=99$ ion beam. Equilibrium intensities of ^{99}Sr γ rays were compared with previously determined absolute γ-ray intensities within the decay chain. A search of the literature[15,25,26] produced absolute intensities for the following γ rays, grouped by parent nucleus: 125.1 keV (^{99}Sr); 121.7 and 724.2 keV (^{99}Y); 469.3, 545.9, and 594.1 keV (^{99}Zr); and 137.6 keV (^{99}Nb). Absolute intensities for the 121.7- and 594.1-keV γ rays were determined in Ref. 25 by comparing relative γ intensities and relative fission yields for mass chains $A=99$ and 91. The rest depend upon the respective $A=99$ level schemes. The values we deduced for β_0, the ^{99}Sr ground-state β feeding, for the γ rays (in keV) were $\sim20\%$ (121.7 and 125.1), $\sim45\%$ (469.3, 545.9, and 594.1), $\sim32\%$ (724.2), and either $\sim27\%$ (137.6) or $\sim43\%$ (137.6). The two values given for 137.6 depend upon the relative population of the two ^{99}Nb isomers following the ^{99}Zr decay.[25,26] There are large uncertainties in each of these values of β_0. For the sake of discussion we have chosen 30% as a rough average of these values.

The β feeding and logft values given in Table II are based on a β_0 of 30%. Due to the uncertainty in this number, we assign to the corresponding logft of 5.0 an asymmetric uncertainty of $+0.5$ and -0.2. The upper uncertainty reflects the fact that the 30% value is more likely to be high than low because of the possibility of missing γ strength directly to the ground state in our decay scheme. It should be noted that those conclusions in this paper based on logft values would not be altered even if β_0 were as low as 10%.

Spin and parity assignments for levels below 1.3 MeV are based on model dependent arguments and are dis-

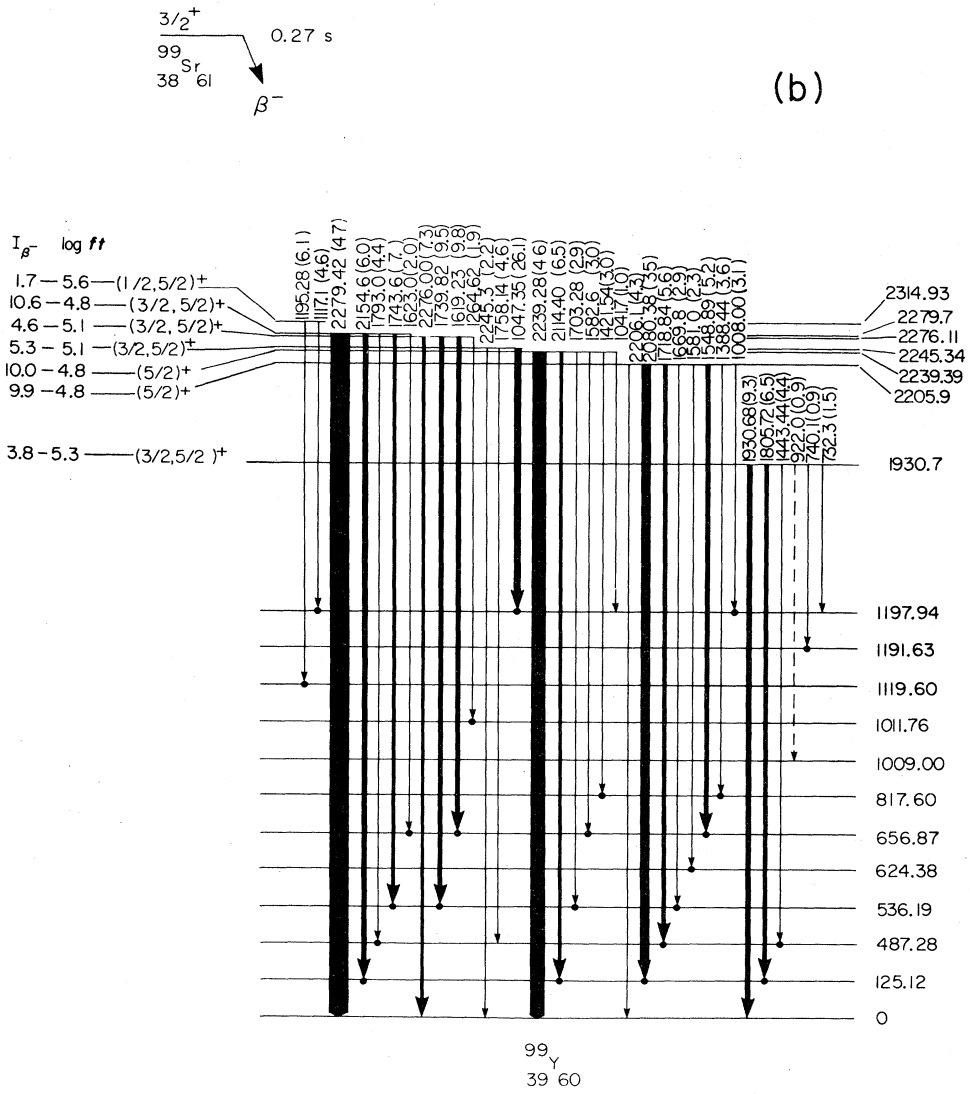

FIG. 5. (*Continued*).

cussed in Sec. IV. The assignment of $\frac{5}{2}^+$ to the ^{99}Y ground state[1] and the low logft for the ground state β decay from ^{99}Sr limits the I^π of the ^{99}Sr ground state to $\frac{3}{2}^+$, $\frac{5}{2}^+$, or $\frac{7}{2}^+$. Results from the decay of ^{99}Rb strongly support a $\frac{3}{2}^+$ assignment for this level,[1] and we shall assume $\frac{3}{2}^+$ in all subsequent discussion.

A striking feature of the ^{99}Y level scheme is a cluster of five states between 2.2 and 2.3 MeV which account for $\sim$40% of the observed β feeding ($\sim$60% of β feeding to excited states). The logft values for all levels above 1.9 MeV are less than 5.8, implying that the β transitions are allowed. This requires that the I^π assignments of these levels be limited to $\frac{1}{2}^+$, $\frac{3}{2}^+$, or $\frac{5}{2}^+$. The $\frac{1}{2}^+$ choice can be excluded for the levels at 1930, 2205, 2239, and 2279 keV, since these levels decay to the $\frac{7}{2}^+$ level at 125 keV. In addition, levels at 2205 and 2239 keV decay to $\frac{7}{2}^-$ states which also excludes a $\frac{3}{2}^+$ assignment. The $\frac{1}{2}^+$ assignment is also excluded for levels at 2245 and 2276 keV, since we observe a γ decay to a $\frac{5}{2}^-$ state which would be $M2$. The I^π for the 1402 keV level is limited to $\frac{3}{2}^+$ or $\frac{5}{2}^\pm$ since it decays to the $\frac{7}{2}^+$ level at 125 keV. I for the 1411-keV level is limited to $\frac{1}{2}$, $\frac{3}{2}$, or $\frac{5}{2}$ based on its value for the logf_1t of 7.8.

IV. DISCUSSION

A. Rotational bands in ^{99}Y

Five rotational bands have been identified in ^{99}Y. These bands are shown in Fig. 6. Below an excitation energy of 1.3 MeV, all levels except those at 599 and 1197 keV belong to the above rotational bands. Table III gives some of the quantities that characterize the five observed bands. In this subsection the band assignments, a simple empirical analysis of the level energies of each band, and a qualitative discussion of the properties of the transitions observed from these levels is presented. A quantitative

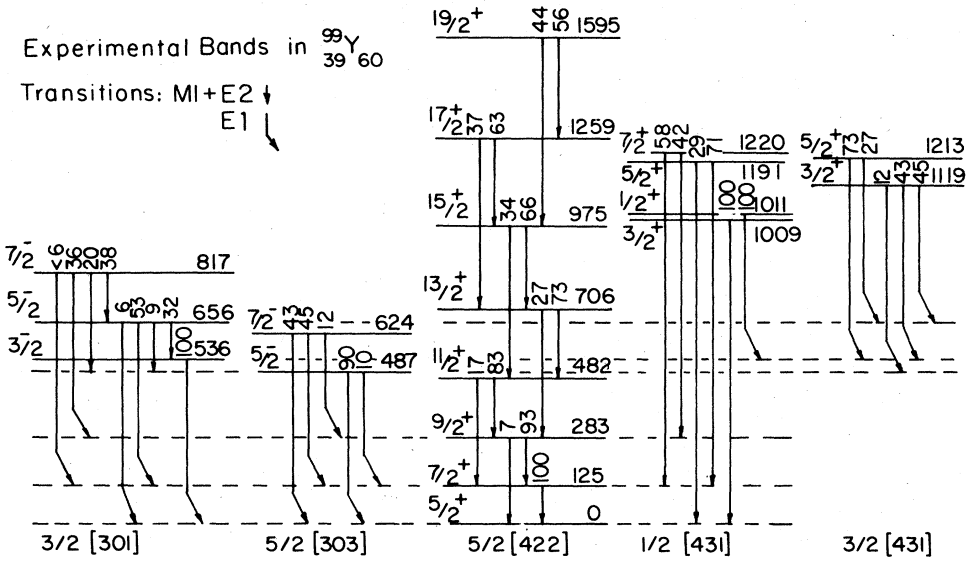

FIG. 6. Experimentally determined Nilsson bands and relative transition intensities for ^{99}Y.

analysis of the level energies and transition probabilities is presented in the following paper, which is referred to hereafter as paper II.

A Nilsson diagram (calculated with the usual harmonic oscillator potential) appropriate for protons with $Z\sim 40$ and $N\sim 60$ is given in Fig. 7. For the Nilsson parameters κ in the range 0.066—0.070 and μ in the range 0.52—0.55 the Nilsson diagram reproduces the experimental single-particle energy ordering and spacing for the spherical Y nuclei near stability. (As is discussed in paper II, the specific choices $\kappa=0.067$ and $\mu=0.534$ best reproduce the five observed bandhead energies of ^{99}Y.) For the deformation δ of about 0.35, the Fermi level for $Z=39$ should lie nearest to the $\frac{5}{2}[422]$ orbital. The next four orbitals nearest to the Fermi level are $\frac{5}{2}[303]$, $\frac{3}{2}[301]$, $\frac{1}{2}[431]$, and $\frac{3}{2}[431]$. Other choices[8,9,11] of a deformed potential well, such as the Wood-Saxon well of Ref. 8, do not alter the conclusion that these five Nilsson orbitals, which we have observed in ^{99}Y, should occur at or near the Fermi level for $Z=39$ and axially symmetric deformations in the range 0.3—0.4. The energy levels and deexcitation patterns determined experimentally were thus examined and found to provide consistent evidence of rotational bands built upon these Nilsson orbitals.

For an axially symmetric rotor, the level energies can be written, in terms of the quantity $J^2=I(I+1)-K(K+1)$, as

$$E_{I,K}=E_{K,K}+aJ^2+bJ^4 +a_{2K}[(-)^{I+K}(I+K)!/(I-K)!-(-)^{2K}(2K)!]\ ,$$

where $E_{K,K}$ is the bandhead energy, a is the inertial parameter $\hbar^2/2\mathscr{I}$, b is due to the rotation-vibration and rotation-particle couplings, and a_{2K} (the so-called signature term) is due to the rotation-particle (Coriolis) coupling. (This equation is rewritten from Ref. 14 in order to have the bandhead energy appear explicitly.) For $K=\frac{1}{2}$, a_1/a is the usual decoupling parameter. For a nearly rigid rotor, b should be negative, both b and a_{2K} (if $K\neq\frac{1}{2}$) should be small compared to a, and the value of K can be determined from the level energies.[14]

For the ground band of ^{99}Y, only $K=\frac{5}{2}$ gives a good fit to the energy levels.[1] For the other four bands, with fewer levels populated in the decay of ^{99}Sr, it was assumed that b and a_{2K} were negligibly small in deducing the value of a. For the $K=\frac{1}{2}$ band, however, a decoupling parameter of ~ -1.0 can be inferred from the near degeneracy of level pairs such as $\frac{1}{2}$ and $\frac{3}{2}$. The values of a shown in Table III show a significant variation. As is shown in paper II, these variations in a can be completely explained in terms of Coriolis mixing of bands. The empirical values of a in Table III should thus be regarded as effective values obtained with the "first-order" assumption of pure-K bands.

In Ref. 1, experimental results were given for the quantity $|(g_K-g_R)/Q_0|$ for the ground-state band in ^{99}Y, where g_K is the intrinsic g factor, g_R is the collective g factor, and Q_0 is the intrinsic quadrupole moment. Under the first-order assumption of a pure-K band, the intraband transition rates depend only on this parameter. Experimental intraband intensity ratios can be used to deduce an effective value of $|(g_K-g_R)/Q_0|$. In Ref. 1 such deduced values were compared with calculated values. The $\frac{5}{2}[422]$ assignment of the ground-state band of ^{99}Y (and the very similar band in ^{101}Y) is strongly supported by such a comparison.[1] For the other bands in ^{99}Y, however, there is insufficient intraband data to analyze each band in this manner. In paper II, a consistent quantitative explanation of all intraband and interband transitions, $E1$ as well as $M1+E2$, is given. In the following discussion, the observed transition patterns are

TABLE II. Level information for ^{99}Y.

Level energy (keV)	Branching[a] (%)	logft[b]
0	30	5.0
125.12±0.04		
283.72±0.05		
482.3 ±0.2		
487.28±0.06		
536.19±0.07	2.0±1.3	6.0
599.99±0.16	2.1±0.3	6.0
624.38±0.09		
656.87±0.06		
817.60±0.05		
1009.00±0.19	1.6±0.2	6.0
1011.76±0.06		
1119.60±0.05		
1191.63±0.33	1.6±0.2	5.9
1197.94±0.16	4.2±0.8	5.5
1213.07±0.10		
1220.65±0.10		
1402.1 ±0.3	2.2±0.3	5.7
1411.69±0.10	2.1±0.3	5.7
1930.7 ±0.2	3.8±0.4	5.3
2205.9 ±0.2	9.9±1.2	4.8
2239.39±0.16	10.0±1.2	4.8
2245.34±0.09	5.3±0.6	5.1
2276.11±0.12	4.6±0.6	5.1
2279.7 ±0.3	10.6±1.3	4.8
2314.93±0.18	1.7±0.3	5.6

[a]Branchings $\lesssim 1.5\%$ are considered unreliable and are omitted. The branchings listed thus sum to less than 100%.

[b]The logft uncertainties are due to the uncertainty in the ground state branching (see the text) and/or unobserved γ rays. We thus judge the logft uncertainties to be ~ 0.3, except for the ground state (see the text).

used to draw qualitative conclusions about the first-order transition strengths. These conclusions are summarized in Table III.

$\frac{5}{2}$[422] band. With $E_{K,K}$ set to zero, fitting the seven excited states[20] gives $a=17.892$ keV, $b=-0.0047$ keV, and $a_{2K}=0.000\,10$ keV, and the rms deviation between experimental and fitted levels is 1.8 keV. This band was also fit to the energy level expression assuming $K=\frac{3}{2}$ and $\frac{7}{2}$. For $K=\frac{3}{2}$ the resulting value of a is ~ 25 keV, the value of b is -0.1 keV, and the fit is quite poor. Since the effective value of a for the lowest band of an odd-A nucleus is reduced from the core value due to Coriolis coupling, the $K=\frac{3}{2}$ fit implies a core value greater than 25 keV, whereas the neighboring even-even nuclei ^{98}Sr or ^{100}Sr have smaller values of a. For $K=\frac{7}{2}$ the fit gives $a=13.6$ keV. This small value of a implies a moment of inertia that is significantly larger than the rigid moment of inertia.

In Ref. 1, the $\frac{5}{2}$[422] assignment for the ground-state band of ^{99}Y was shown to be consistent with the observed intraband transition ratios. Experimentally deduced values of the parameter $|(g_K-g_R)/Q_0|$ were compared with calculated values for the two $K=\frac{5}{2}$ possibilities, $\frac{5}{2}$[422] and $\frac{5}{2}$[303]. As is obvious from comparing the calculated values shown in Fig. 8 (Fig. 3 of Ref. 1) with the experimental value of this parameter, only the $\frac{5}{2}$[422] choice survives this test of intraband transition intensities. The experimental value[1] of this parameter is 0.27 ± 0.03, which implies an $E2/M1$ mixing ratio δ^2 of ~ 0.01 for the low spin members of the band.

The 30% β branch (log$ft=5.0$) to the ground state implies a positive parity for the ^{99}Sr ground state. ^{99}Sr is also deformed, with a ground-state rotational band with $K=\frac{3}{2}$.[1] The experimental intraband transition ratios for this band could not distinguish between the two Nilsson orbital choices $\frac{3}{2}$[411] and $\frac{3}{2}$[541].[1] The strong β branch reported here for the decay of ^{99}Sr, however, provides a clear choice of $\frac{3}{2}$[411]. This low logft β decay is dominated by the Gamow-Teller transition from the $1g_{7/2}$ component (in the Nilsson wave function) for the odd neutron in ^{99}Sr to the $1g_{9/2}$ component for the odd proton in ^{99}Y.

The ground-state logft value of ~ 5.0 (actually in the range 4.8—5.5 as discussed in Sec. III) is unusually low for a β decay that is classified, according to the dominant Nilsson orbitals, as allowed hindered.[14] [In allowed unhindered β decays the quantum numbers $(Nn_z\Lambda)$ do not change.] In the rare-earth region, logft values of ~ 5.5 have been deduced for two allowed hindered (bandhead-to-bandhead) β decays in which the Nilsson orbital $\nu\frac{3}{2}$[521] to $\pi\frac{5}{2}$[532] (^{155}Sm to ^{155}Eu) and $\pi\frac{7}{2}$[523] to $\nu\frac{5}{2}$[512] (^{159}Ho to ^{159}Dy) of the odd nucleon is described by an allowed hindered β decay.[26] These two cases are similar to the present case of $\nu\frac{3}{2}$[411] to $\pi\frac{5}{2}$[422] in that unique-parity orbitals are involved and the asymptotic quantum numbers n_z and Λ both change by unity. In terms of the spherical shell-model components, the dominant orbitals involved are $\pi 1h_{11/2}$ and $\nu 1h_{9/2}$ for the rare earths and $\pi 1g_{9/2}$ and $\nu 1g_{7/2}$ for the $A\sim 100$ nuclei. In these cases the Nilsson orbitals with major components of these spherical states lie near the Fermi surfaces in both of the odd-A nuclei connected by the β decay. The low logft of 5.0 reported here is thus reasonable. This would be the lowest logft yet observed for an allowed hindered β decay, but because of the large uncertainty in this value we hesitate to make this claim.

$\frac{5}{2}$[303] band. As Fig. 6 shows, two levels ($\frac{5}{2}^-$ at 487 keV and $\frac{7}{2}^-$ at 624 keV) are assigned to a $\frac{5}{2}$[303] band. The weak ($<1.5\%$) β feeding of these levels are consistent with the $\frac{5}{2}$[303] assignment. The intraband transition between these two levels is too weak to be observed in either singles or coincidence spectra. Instead, all possible $E1$ transitions to the ground band are observed. As indicated in Table III, $E1$ transitions dominate $M1+E2$ transitions, and $E2$ transitions are expected to dominate $M1$. The reason for the latter is that the two g factors g_K and g_R are expected to be nearly equal for this intrinsic Nilsson state. Figure 8 shows the small value of $(g_K-g_R)/Q_0$ for $\frac{5}{2}$[303]. The explicit inclusion of Coriolis mixing (see paper II) does not alter the $\lambda_{E2}\gg\lambda_{M1}$ feature of this band. This feature, which is also indicated by the intraband transitions reported in Ref. 22 for the $\frac{5}{2}$[303] band in ^{103}Nb, provides a clear distinction between the two $K=\frac{5}{2}$ bands, $\frac{5}{2}$[422] and

TABLE III. Experimental quantities characterizing the observed rotational bands in ^{99}Y.

Nilsson orbital	Bandhead energy (keV)	$a=\hbar^2/2\mathcal{I}$ (keV)	$(2K)!a_{2K}/a$	Pattern of γ-ray deexcitations
$\frac{5}{2}$[422]	0	17.89	6.7×10^{-4}	$\lambda_{M1}\gg\lambda_{E2}$
$\frac{5}{2}$[303]	487	~19.6		$\lambda_{E1}\gg\lambda_{E2}\gg\lambda_{M1}$[a]
$\frac{3}{2}$[301]	536	~23.6		λ_{E1}[b] $\sim\lambda_{M1}\gg\lambda_{E2}$
$\frac{1}{2}$[431]	1011	~17.8	~-1	$\lambda_{M1}\gg\lambda_{E1},\lambda_{E2}$
$\frac{3}{2}$[431]	1119	~23.6		λ_{E1}[c] $\gg\lambda_{M1,E2}$

[a] $\lambda_{M1}\ll\lambda_{E2}$ for the $\frac{5}{2}$[303] band implies that the effective $(g_K-g_R)/Q_0\sim0$.

[b] $\lambda_{E1}\sim\lambda_{M1}$ for the $\frac{3}{2}$[301] band due to hindrance of this $\Delta K=1$ $E1$ strength.

[c] $\lambda_{E1}\gg\lambda_{M1}$ for the $\frac{3}{2}$[431] band requires a strong enhancement of this $\Delta K=0$ $E1$ strength.

$\frac{5}{2}$[303]. As paper II shows, the differences in the observed transition patterns for the $\frac{5}{2}$[303] bands in these two nuclei are a natural consequence of the differences in the Fermi levels and quasiparticle energies.

$\frac{3}{2}$[301] band. Three levels ($\frac{3}{2}^-$ at 536 keV, $\frac{5}{2}^-$ at 656 keV, and $\frac{7}{2}^-$ at 817 keV) of the $\frac{3}{2}$[301] band are observed in the decay of ^{99}Sr. All possible types of transitions are observed: intraband $M1+E2$, interband $M1+E2$, and interband $E1$. The intraband transitions indicate $\lambda_{M1}\gg\lambda_{E2}$ and the interband $E1$ transition intensities indicate $\lambda_{E1}\sim\lambda_{M1}$. This latter feature restricts the relative strengths of the $E1$ and $M1$ transitions in the calculations given in paper II. The $\frac{3}{2}$[301] band has been identified in ^{103}Nb (Ref. 22) and the intraband transitions also give a clear indication that $\lambda_{M1}\gg\lambda_{E2}$.

$\frac{1}{2}$[431] band. Four levels, $\frac{1}{2}^+$ at 1011 keV, $\frac{3}{2}^+$ at 1009 keV, $\frac{5}{2}^+$ at 1192 keV, and $\frac{7}{2}^+$ at 1220 keV, can be assigned to a $\frac{1}{2}$[431] band. Since the $\frac{3}{2}^+$ level is slightly below the $\frac{1}{2}^+$ level, the decoupling parameter for this band appears to be slightly more negative than -1.0, which should cause the $\frac{7}{2}^+$ level to lie below the $\frac{5}{2}^+$ level. The fact that it does not indicates that levels in this energy range are likely to be highly admixed. This should be particularly true for $\frac{5}{2}^+$ levels, as we have postulated three $\frac{5}{2}^+$ levels near 1.2 MeV. For bands above ~1 MeV, three-quasiparticle (or one-quasiparticle states coupled to β or γ core vibrations) bands could be expected to mix with one-quasiparticle bands. Thus significant violations to the simple first-order one-quasiparticle energy and intensity predictions can be expected.

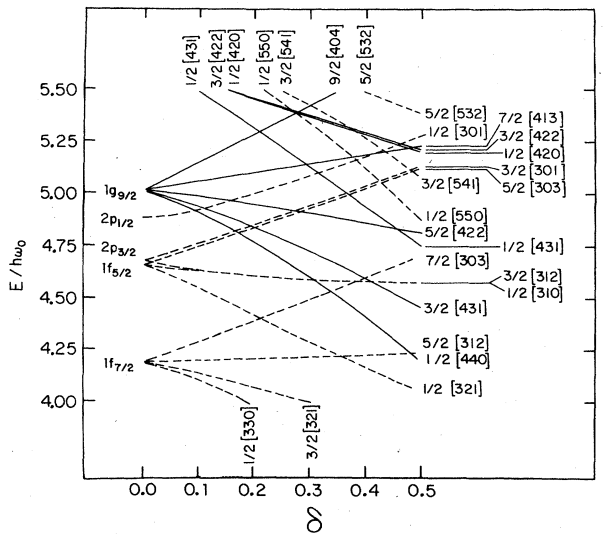

FIG. 7. Nilsson diagram for protons for $\kappa=0.067$ and $\mu=0.534$.

Except for the $E1$ transition from the $\frac{1}{2}^+$ bandhead to the $\frac{3}{2}^-$ level at 536 keV, the members of the proposed $\frac{1}{2}$[431] band appear to deexcite by $M1$ transitions to the $\frac{5}{2}$[422] ground band. If these were pure-K bands, these would be forbidden $\Delta K=2$ transitions, yet they are observed and no $\Delta K=1$ $E1$ transitions are observed (except from the $\frac{1}{2}^+$ bandhead). This deexcitation pattern can be understood only if the $\Delta K=1$ $E1$ transitions are hindered and if unhindered $\Delta K=1$ $M1$ transitions between Coriolis-mixed components in the $\frac{1}{2}$[431] or $\frac{5}{2}$[422] bands are significant. The quantitative analysis of transition rates in paper II for Coriolis-mixed one-quasiparticle states shows that this explanation is indeed plausible.

$\frac{3}{2}$[431] band. Two levels, $\frac{3}{2}^+$ at 1119 keV and $\frac{5}{2}^+$ at 1213 keV, are proposed for a $\frac{3}{2}$[431] band. This band assignment is more tentative than the others and is more model dependent. According to the Nilsson diagram, the $\frac{3}{2}$[431] bandhead should occur at an excitation energy close to that for the $\frac{1}{2}$[431] bandhead. The comments made above, concerning possible admixtures of bands based on either three-quasiparticle or one-quasiparticle states coupled to core vibrations, apply to the $\frac{3}{2}$[431] as well as the $\frac{1}{2}$[431] band.

The two levels of this band have a deexcitation pattern of $\Delta K=0$ $E1$ transitions dominating (unobserved) $M1$ transitions. This implies an enhancement of the $E1$ strength for $\frac{3}{2}$[431] to $\frac{3}{2}$[301] transitions which is large enough to dominate the $\Delta K=1$ $M1$ transitions. The latter transition strength, if approximated from the pure-K band $\frac{3}{2}$[431] to $\frac{5}{2}$[422] single-particle $M1$ strength[30] (the interband equivalent of the parameter g_K-g_R)

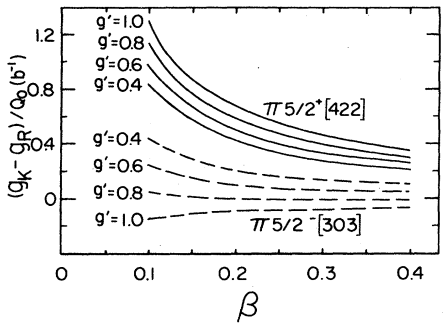

FIG. 8. Calculated values of $(g_K-g_R)/Q_0$ for two of the $K=\frac{5}{2}$ Nilsson proton orbitals. $g_R\simeq Z/A=0.39$, $g'=g_s^{\text{effective}}/g_s^{\text{free}}$, and $Q_0=9.2\beta(1+0.16\beta)$ for ^{99}Y. β and the Nilsson deformation parameter δ are related by $\beta=\frac{4}{3}(\pi/5)^{1/2}\delta(1+\frac{1}{2}\delta+\frac{1}{2}\delta^2+\cdots)$.

should not be significantly hindered. As is shown by the one-quasiparticle calculations given in paper II, the deexcitation pattern for this proposed band cannot be reproduced by one-quasiparticle calculations, but requires a strong enhancement of the $E1$ strength. Designation of this band as $\frac{3}{2}[431]$ is thus more tentative than the other band assignments.

In a review of $E1$ strengths,[31] the general trend is for $\Delta K\neq 0$ $E1$ transitions to be more hindered than $\Delta K=0$ $E1$ transitions. This general tendency appears to occur for $E1$ transitions in ^{99}Y, as they are dominant for the two $\Delta K=0$ cases but not dominant for the two $\Delta K=1$ cases.

B. Other levels in ^{99}Y

599-keV level. The level at 599 keV is the only level below 1.2 MeV not associated with a one-quasiparticle rotational band. Only one transition (63 keV to the $\frac{3}{2}^-$ level at 536 keV) deexcites this level and only one transition (802 keV from the level at 1402 keV) is observed to populate it. (A level at an energy of 620 keV in ^{103}Nb was reported in Ref. 22 as the only level below $\sim$0.7 MeV not associated with one of the three rotational bands identified in ^{103}Nb.) In the neighboring even-even nuclei ^{98}Sr and ^{100}Zr, exceptionally low-lying 0^+ states have been observed. These 0^+ states have been attributed to shape coexistence in these $N=60$ nuclei, with nearly spherical states coexisting with well-deformed rotational states.[32,33] Since the energy difference of $\sim$0.8 MeV between the 599- and 1402-keV states in ^{99}Y is similar to the 2_1^+ energy of $\sim$0.8 MeV in the spherical Sr nuclei, it is interesting to speculate that the states in ^{99}Y at 599 and 1402 keV may be associated with a spherical shape in this $N=60$ nucleus.

1197-keV level. Other than the ground state, the 1197-keV level is the only one below 1.9 MeV with significant β feeding. The low logft of 5.5 for this level indicates an allowed β transition, hence the spin-parity choices are $\frac{1}{2}^+$, $\frac{3}{2}^+$, or $\frac{5}{2}^+$. Of these, the most likely spin choice is $\frac{5}{2}^+$. The strong γ-ray transition to the ground state would be expected for a $\frac{5}{2}^+$ state at 1197 keV if it has a significant component of a particle-vibration wave function corresponding to $\frac{5}{2}[422]$ coupled to the 0^+ first β vibration. (As stated earlier, the $\frac{1}{2}[431]$ band could contain an appreciable fraction of $\frac{5}{2}[422]$ coupled to the 2^+ first γ vibration.) With $\frac{5}{2}^+$ states at 1191, 1197, and 1213 keV, mixing would be expected. If the 1197 keV level consists mainly of $\frac{5}{2}[422]$ coupled to the first β vibration, then, in order to explain the low logft, one of the three-quasiparticle states comprising its wave function should be such that an allowed unhindered β transition can occur.[14]

Levels around 2.2 MeV. A possible interpretation of these low logft levels is a three-quasiparticle state in ^{99}Y that could be fed by an allowed unhindered β transition from the $\nu\frac{3}{2}[411]$ ground state of the deformed $N=61$ parent nucleus ^{99}Sr. Likely three-quasiparticle configurations are

$$\{\pi\tfrac{5}{2}[422],\nu\tfrac{3}{2}[411],(\nu\tfrac{3}{2}[422])^{-1}\}_I$$

with $I=\frac{1}{2}$, $\frac{3}{2}$, and $\frac{5}{2}$. The allowed unhindered Gamow-Teller β transition $\nu\frac{3}{2}[422]\rightarrow\pi\frac{5}{2}[422]$ would explain the low logft values. (The orbital $\nu\frac{3}{2}[411]$ lies below the Fermi level in ^{99}Sr, hence it is nearly fully occupied by two neutrons.) Unhindered single-particle $M1$ transitions $\nu\frac{3}{2}[411]\rightarrow\nu\frac{3}{2}[422]$ would explain the strong γ-ray transitions to members of the $\pi\frac{5}{2}[422]$ ground-state band.

Alternatively, these levels may involve β and γ vibrations coupled to the $\frac{5}{2}[422]$ ground state. It is intriguing to note in this vein that the cluster of five levels is located at about twice the energy of the 1197-keV level. If the levels around 2.2 MeV contain admixtures of $\frac{5}{2}[422]$ coupled to the 0^+ second β vibration, then the γ-ray strength to the 1197-keV level would consist of a "one-phonon transition" to the first-β vibrational component of the latter level. The level at 2245 keV, which has 80% of its γ-ray strength to the 1197-keV level, would have most of the second-β vibration in its composite wave function. The signature of the other levels around 2.2 MeV is not as simple, hence it is unclear whether a three-quasiparticle or vibrational coupling interpretation is preferable.

ACKNOWLEDGMENTS

The authors wish to express their appreciation to the U.S. Department of Energy for the support that has made the work possible. The non-BNL authors also wish to express their appreciation to the neutron-nuclear physics group at BNL for continued hospitality during the course of this work, strong technical support for the experimental work, and incisive discussions with Dr. R. F. Casten and Dr. D. D. Warner.

*Present address: Cyclotron Institute, Texas A&M University, College Station, TX 77843.

†Present address: ELTA Electronics Industries Ltd, Ashdod, Israel.

[1]F. K. Wohn, J. C. Hill, R. F. Petry, H. Dejbakhsh, Z. Berant, and R. L. Gill, Phys. Rev. Lett. **51**, 873 (1983).

[2]D. A. Arseniev, A. Sobieczewski, and V. G. Soloviev, Nucl. Phys. **A139**, 269 (1969).

[3]E. Cheifetz, R. C. Jared, S. G. Thompson, and J. B. Wilhelmy, Phys. Rev. C **4**, 1913 (1971).

[4]E. Cheifetz, H. A. Selic, A. Wolf, R. Chechik, and J. B. Wilhelmy, in *Nuclear Spectroscopy of Fission Products,* IOP Conf. Series. Vol. 51, edited by T. von Egidy (Institute of Physics, London, 1980), p. 193.

[5]K. Sistemich, in *Nuclear Spectroscopy of Fission Products,* IOP Conf. Series Vol. 51, edited by T. von Egidy (Institute of Physics, London, 1980), p. 208.

[6]J. A. Pinston, in *Nuclear Spectroscopy of Fission Products,* IOP Conf. Series. Vol. 51, edited by T. von Egidy (Institute of Physics, London, 1980), p. 528.

[7]J. Stachel, N. Kaffrel, E. Grosse, H. Emling, H. Folger, R. Kulessa, and D. Schwalm, Nucl. Phys. **A383**, 429 (1982).

[8]A. Faessler, J. E. Galonska, U. Gota, and H. Pauli, Nucl. Phys. **A230**, 302 (1974).

[9]S. Mattsson, R. E. Azuma, H. A. Gustafsson, P. G. Hansen, B. Jonson, V. Lindfora, G. Nyman, I. Ragnarsson, H. L. Ravn, and D. Schardt, in *Proceedings of the Fourth International Conference on Nuclei Far from Stability, Helsingør, Denmark, 1981,* edited by P. G. Hansen and O. B. Nielson (CERN, Geneva, 1981), p. 430.

[10]P. Tondeur, Nucl. Phys. **A359**, 278 (1981).

[11]R. Bengtsson, P. Möller, J. R. Nix, and J. Zhang, Phys. Scr. **29**, 402 (1984).

[12]J. Stachel, P. Van Isacker, and K. Heyde, Phys. Rev. C **25**, 650 (1982).

[13]P. Federman and S. Pittel, Phys. Rev. C **20**, 820 (1979).

[14]M. E. Bunker and C. W. Reich, Rev. Mod. Phys. **43**, 348 (1971).

[15]B. Pfeiffer, E. Monnand, J. A. Pinston, F. Schussler, G. Jung, J. Munzel, and H. Wollnik, in *Proceedings of the Fourth International Conference on Nuclei Far From Stability, Helsingør, Denmark, 1981,* edited by P. G. Hansen and O. B. Nielsen (CERN, Geneva, 1981), p. 423.

[16]M. Epherre, G. Audi, C. Thibault, R. Klapisch, G. Huber, F. Touchard, and H. Wollnik, Phys. Rev. C **19**, 1504 (1979).

[17]H. E. Duckworth, R. C. Barber, P. Van Rookhuysen, J. D. MacDougall, W. McLatchie, S. Whineray, R. L. Bishop, J. O. Meredith, P. Williams, G. Southon, W. Wong, B. G. Hogg, and M. E. Kettner, Phys. Rev. Lett. **23**, 592 (1969).

[18]C. Thibault, R. Klapisch, C. Rigaud, A. M. Poskanzer, R. Prieels, L. Lessard, and W. Reisdorf, Phys. Rev. C **12**, 644 (1975).

[19]C. Thibault, F. Touchard, S. Büttgenbach, R. Klapisch, and M. de Saint Simon, H. T. Duong, P. Jacquinot, P. Juncar, S. Liberman, P. Pillet, J. Pinard, A. Pesnelle, and G. Huber, Phys. Rev. C **23**, 2720 (1981).

[20]E. Monnand, J. A. Pinston, F. Schussler, B. Pfeiffer, H. Lawin, G. Battistuzzi, K. Shizuma, and K. Sistemich, Z. Phys. A **306**, 183 (1982).

[21]K. Shizuma, H. Ahrens, J. P. Bocquet, N. Kaffrell, B. D. Kern, H. Lawin, R. A. Meyer, K. Sistemich, G. Tittel, and N. Trautmann, Z. Phys. A **315**, 65 (1984).

[22]T. Seo, A. M. Schmitt, H. Ahrens, J. P. Bocquet, N. Kaffrell, H. Lawin, G. Lhereonneau, R. A. Meyer, K. Shizuma, K. Sistemich, G. Tittle, and N. Trautmann, Z. Phys. A **315**, 251 (1984).

[23]M. Shmid, R. L. Gill, and C. Chung, Nucl. Instrum. Methods **211**, 287 (1983).

[24]H. G. Börner, W. F. Davidson, J. Almeida, J. Blachot, J. A. Pinston, and P. H. M. Van Assache, Nucl. Instrum. Methods **164**, 579 (1979).

[25]H. A. Selic, G. Sadler, T. A. Kahn, W. D. Lauppe, H. Lawin, K. Sistemich, E. Monnand, J. Blachot, J. P. Bocquet, and F. Schussler, Z. Phys. A **289**, 197 (1979).

[26]*Tables of Isotopes,* 7th ed., edited by C. M. Lederer and V. S. Shirley (Wiley, New York, 1978), p. 424.

[27]E. Koglin, G. Jung, G. Siegert, R. Decker, K. D. Wünsch, and H. Wollnik, Z. Phys. A **288**, 319 (1978).

[28]M. Asghar, J. P. Gautheron, G. Bailleul, J. P. Bocquet, J. Greif, M. Schrader, G. Siegert, C. Ristori, J. Crancon, and G. I. Crawford, Nucl. Phys. A **247**, 359 (1975).

[29]R. Iafigliola (private communication).

[30]E. Browne and F. R. Femenia, Nucl. Data Tables **10**, 81 (1971).

[31]C. F. Perdrisat, Rev. Mod. Phys. **38**, 41 (1966).

[32]T. A. Khan, W.-D. Lauppe, K. Sistemich, H. Lawin, and H. A. Selic, Z. Phys. A **284**, 313 (1978).

[33]F. Schussler, J. A. Pinston, E. Monnand, A. Moussa, G. Jung, E. Koglin, B. Pfeiffer, R. V. F. Janssen, and J. van Klinken, Nucl. Phys. **A339**, 415 (1980).